Cutter Load Distribution Analysis and Crown Shape Optimal Design of Complex Curved PDC Bit

Ju Pei

Xi'an Research Institute of China Coal Technology & Engineering Group Corp, Xi'an, China
E-mail: jpnt2005@163.com

Abstract. When drilling in hard rock formations, the wear of the complex curved PDC bit is extremely uneven. To solve this problem, a numerical simulation method was used to analyze the load distribution law of the cutters and the crown shape of the complex curved PDC bit was optimized. The simulation results showed that: 1) along the radial direction of the bit, the axial load on the cutters increased first and then decreased, while the radial load decreased first and then increased; 2) the axial load on the cutters was the largest at the nose and taper area of the bit, while the radial load on the cutters was the largest at the center and shoulder area of the bit; 3) the influence of the inner cone angle on the cutting load was mainly concentrated in the bit crown's inner cone area, while the influence of the outer arc radius on the cutting load was mainly concentrated in the bit crown nose and taper areas. Based on these conclusions, the crown shape of the complex curved PDC bit was optimized and a field test was carried out. The test results showed that, compared with the original complex curved PDC bit, the average bit life and drilling efficiency of the new designed bit was increased by 20% and 18%, respectively, especially in hard rock drilling. The average drilling efficiency of the new designed bit was increased by 50%.

Keywords: *complex curved PDC bit; crown shape design; field test; hard rock drilling; numerical simulation.*

1 Introduction

With the development of drilling technology in coal drilling engineering, the drilled formation situation is increasingly complex. High degrees of hardness and abrasive rocks are often encountered, which makes the wear of the concave PDC bit become more and more serious, as shown in Figure 1(a) [1]. To solve this problem, a complex curved PDC bit was developed, as shown in Figure 1(b). A field drilling test of the complex curved PDC bit showed that the drilling efficiency and average bit life of the complex curved PDC bit was increased by more than 30% compared with a concave PDC bit. Especially in hard rock drilling, the complex curved PDC bit can be used to replace the concave PDC bit to improve rock breaking efficiency [2,3].

Received October 18th, 2017, 1st Revision October 8th, 2018, 2nd Revision January 8th, 2019, Accepted for publication January 11th, 2019.
 ISSN: 2337-5779, DOI: 10.5614/j.eng.technol.sci.2019.51.1.2

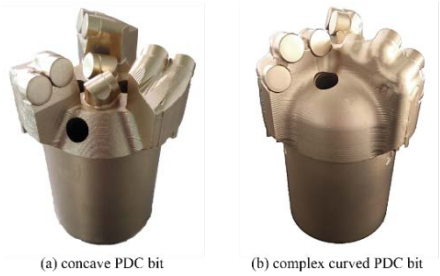

Figure 1 Photograph of concave and complex curved PDC bits.

However, when drilling into a highly heterogeneous formation, the wear of the cutters in each part of the complex curved PDC bit is very uneven. Figure 2 is a photograph of a used complex curved PDC bit, from which it can be seen that the cutters are worn seriously in the bit crown nose area, while the other cutters are still in good condition. The reason can be summarized as follows: when drilling into a hard and heterogeneous formation, the rotation center of the bit will change instantaneously, causing the cutters to bear large impact loads. Hence, some cutters will be damaged sooner than others and the performance of the damaged complex curved PDC bit will be greatly reduced.

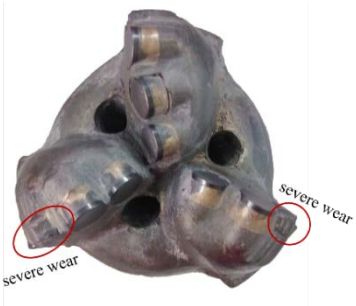

Figure 2 Photograph of used complex curved PDC bit.

To solve the above problems and make the wear of the cutters of the complex curved PDC bit more uniform, the finite element method was adopted to analyze the load distribution law of the cutters. Finally, the crown shape of the bit was optimized so as to give full play to the advantage of high drilling efficiency of the complex curved PDC bit.

2 Finite Element Simulation Model

In recent years, the finite element method has been widely used in the study of rock breaking problems [4-9]. Jaime [10] employed the Lagrangian finite element method in modeling the rock cutting process. The fragmentation

progression obtained from the simulation analysis could capture various fracture phases well, from crack initiation to chip formation, the interaction of the chips, the cutter, and the rock sample. Zhou [11] modeled the groove cutting process with rectangular and disc cutters using the LS-DYNA method. He concluded that the volume of the cut was sensitive to the mesh size. The modeling results were also consistent with the available laboratory test results.

Pryhorovska [12] simulated linear and circular rock cutting processes using the finite element method. The results showed that there was no essential difference between curricular cutting and linear cutting. Jiang [13] investigated the rock fragmentation mechanism and its influence factors under discontinuous water-jet impact using coupled smoothed particle hydrodynamics and the finite element analysis method. The rock failure mechanisms, such as the crushing zone and crack formation, were analyzed through the elements of pressure and stresses as a function of time. Ducobu [14] introduced a 3D finite element Coupled Eulerian-Lagrangian (CEL) model of orthogonal cutting that was verified by comparison with experimental operation. It faithfully reproduced the experimental operation: the force, the chip thickness and the lateral expansion of the chip were accurately modeled.

The rock breaking process is very complicated. There are no explicit analytic solutions, so the finite element method is a good tool for the study of rock-breaking problems. Previous simulation research results have shown essential convergence between experimental and simulated data, so the finite element method can be used to analyze rock-breaking problems in the absence of experimental data.

2.1 Geometric Model

To simplify the calculation, two assumptions were made: 1) the influence of confining pressure, temperature and drilling fluid was ignored; 2) the wear of the cutter was ignored.

Taking a ø94 mm complex curved PDC bit as an example, the cutters were taken as the rock-breaking components of the bit in order to focus on the analysis of the load distribution characteristics of the cutters. The bit's body and blade were ignored during the simulation and only the cutters were taken as research object. The 3D geometric model is shown in Figure 3.

The cutters and rock were modeled using the Solid 164 element. The size of the rock was 140 × 140 × 100 mm and the size of the cutter was ø13.44 × 8 mm. The rock and the cutters were generated on rectangular grids with the grid size

as small as possible to improve the calculation accuracy. The grid sizes of the rock and cutters were 2.5 mm and 1.0 mm respectively.

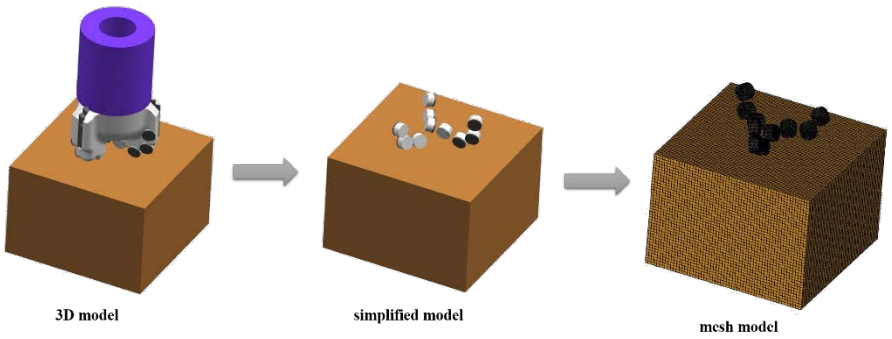

Figure 3 3D finite element model of rock breaking.

2.2 Material Model

The rock was hard and tight sandstone in order to reflect the rock damage process from plastic deformation to damage failure. The material model of the rock was set as an elastic-plastic damage constitutive Cambridge material [15]. The yield surface equation was in Eq. (1) as follows:

$$\frac{1}{\beta^2}\left(\frac{p}{a}-1\right)^2+\left(\frac{t}{Ma}\right)^2-1=0 \tag{1}$$

where $p=-\frac{1}{3}(\sigma_1+\sigma_2+\sigma_3)$, which represents the average compressive stress; $t=\frac{q}{2}[1+\frac{1}{K}-(1-\frac{1}{K})(\frac{r}{q})^3]$, which represents the deviatoric stress; $q=\sqrt{\frac{3}{2}(S:S)}$, which represents the equivalent Von Mises stress; $r=(\frac{9}{2}S\cdot S:S)^{1/3}$, which represents the third stress invariant; M is a constant that defines the slope of the critical state line; a is the hardening index of the material; β is a constant (on the dry side of the critical state line $\beta=1.0$, and on the wet side $\beta\neq1.0$); K is the ratio of yield stress of triaxial tension and triaxial compression, $0.778\leq K\leq1.0$.

The cutting material of the cutter was a polycrystalline diamond layer. Its hardness and strength are far greater than those of the rock. For the sake of improving computational efficiency, the material model of the cutter was set as a rigid material. Table 1 shows the material parameters of the cutters and the rock.

Table 1 Summary of physical parameters.

Material	Density (g/cm3)	Elasticity modulus (Mpa)	Tangent modulus (Mpa)	Poisson's ratio	Compressive strength (Mpa)
Rock	2.1	4E4	0.4E4	0.15	165
Cutter	3.56	8.9E5		0.07	

2.3 Boundary Conditions and Load Applying

All the cutters moved straight down at a constant vertical velocity of 30 m/h. At the same time they rotated around their centerline with a constant speed of 100 r/min. The rock remained stationary. Therefore, all translational and rotational degrees of rock node freedom were fixed and the rotational degrees of cutter node freedom were fixed in the X and Y directions.

The contact friction between the cutter and the rock was based on Coulomb's formula. In order to represent the degradation of the rock's mechanical properties (strength and stiffness) that occurs when an external load is applied to the rock, a two-way treatment of eroding contact was chosen and a penalty contact algorithm was adopted. The contact stiffness was calculated using a soft constraint-based approach.

To avoid the influence of boundary wave reflection, a non-reflecting boundary condition was applied to the rock boundary surface. The cutting process involves large deformations, so in order to overcome the computational difficulties caused by grid distortion, the Arbitrary Lagrangian Eulerian method was used. The Flanagan-Belytschko hourglass viscous damping algorithm was adopted to control the hourglass caused by large deformations to keep the hourglass energy within 10% of the total internal energy.

3 Results and Discussion

The crown shape of the complex curved PDC bit is mainly composed of 'straight line-arc-straight line' or 'straight line-arc-arc' styles, so the bit's crown can be divided into five areas: the inner cone area, the nose area, the taper area, the shoulder and the gauge area. The bit's crown shape can be represented by the parameters inner cone angle α and outer arc radius R [13]. Figure 4 shows the crown structure of the complex curved PDC bit.

Systematically analyzing the simulation results, the characteristics of the load change law of all the cutters were grasped to guide the optimal design of the crown shape of the complex curved PDC bit.

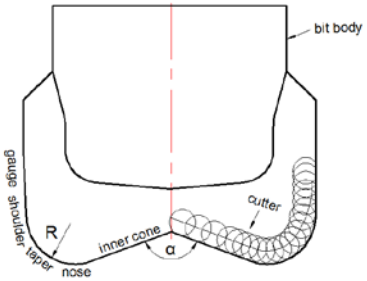

Figure 4 Crown structure of complex curved PDC bit.

3.1 Load Distribution of the Cutters

Figure 5 shows the Von Mises stress state of the rock at some point. The Von Mises stress of the rock element at the nose area is relatively large, which indicates that the load needed to break the rock in this area is large. Because of the limitations of the hexahedral mesh, the formed well wall is not smooth.

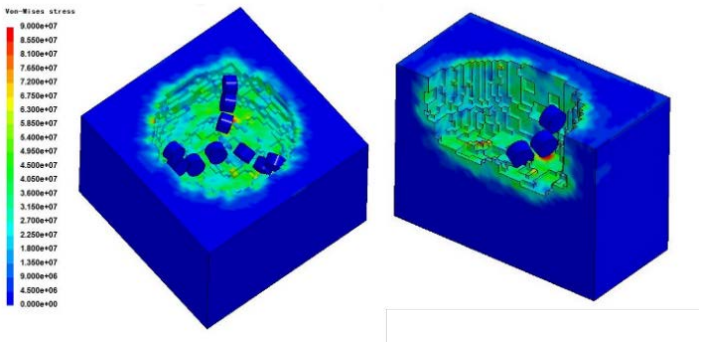

Figure 5 Von Mises stress diagram at some point of the rock.

All the cutters are referred to in the form of ‘a-b’, where ‘a’ represents the number of the blade and ‘b’ represents the number of the cutter. Taking cutter 1-2 as an example: this represents cutter number 2 on blade number 1. All the cutters were placed along the bit’s radial direction in a staggered form. Figure 6 shows the variation law of the axial load of the cutters along the bit’s radial direction.

From Figure 6 it can be seen that along the radial direction of the bit, the axial load on the cutters increased first and then decreased. The cutters at the nose and taper areas bore a large axial load, while the cutters at the inner cone and shoulder areas bore a small axial load. This can be explained by the fact that the cutters at the nose and taper areas have a larger bottom hole curvature, while the

free face of the rock under these cutters is small, which results in the rock in this part being more difficult to break.

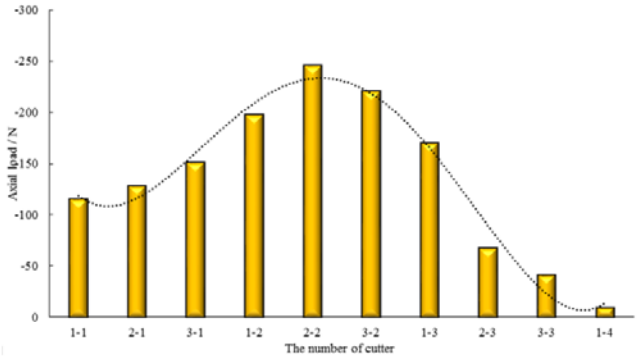

Figure 6 Histogram of the axial load on the cutters along the bit's radial direction.

Figure 7 shows the variation law of the radial load of the cutters along the bit's radial direction. Except for cutters 3-3 and 1-4, the radial load on the cutters in the shoulder and gauge areas decreased first and then increased along the radial direction of the bit. The cutters bore a large radial load in the inner cone and shoulder areas, while they bore a small radial load in the nose and taper areas.

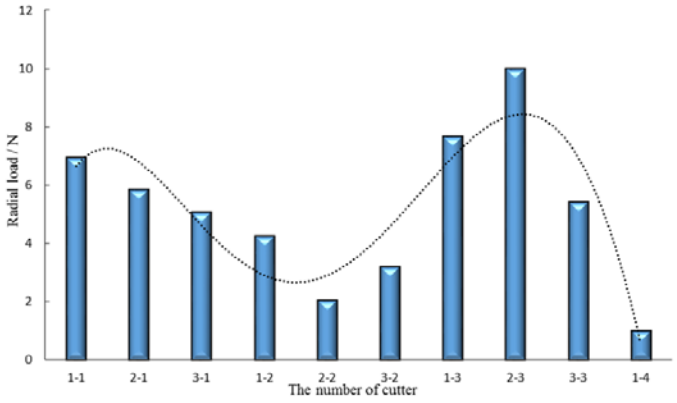

Figure 7 Histogram of the radial load on the cutters along the bit's radial direction.

This is because the cutters in the inner cone and shoulder areas have a smaller bottom hole curvature. The movement freedom of the rock under these cutters is large, so the radial unbalanced load on these cutters is large. Meanwhile, the

cutters bore large constraints in the nose and taper areas from the rock, so the radial movement of these cutters was small.

3.2 Crown Shaped Optimal Design of Complex Curved PDC Bit

From Figures 6 and 7 it can be seen that, because of the restriction of the crown shape of the complex curved PDC bit, the load on the cutters was not uniform. The axial load on the cutters was larger in the nose and taper areas, while the radial load of the cutters was larger in the inner cone and shoulder areas.

By optimizing the design of the crown shape of the complex curved PDC bit, the load distribution condition on the cutters can be improved and the occurrence of very uneven load distribution can be avoided. From the above analysis, the crown shape of the complex curved PDC bit can be represented by inner cone angle α and outer arc radius R, so analyses of the effects of α and R on the load distribution of the cutters were carried out.

3.2.1 Influence of Inner Cone Angle on Cutter Load

The control variable parameter method was used, leaving the outer arc radius of 20 mm unchanged while the inner cone angle was taken as 160°, 150°, 140° and 130°, respectively. Figure 8 shows a histogram of the axial load on the cutters along the radial direction of the bit at different inner cone angles. From Figure 8 it can be seen that cutters 2-2 and 3-2 bore maximal axial load. With the decrease of the inner cone angle, the axial load on cutters 1-1, 2-1, 3-1 and 1-2 decreased gradually in the inner cone area. In all programs, the axial load on the cutters was the same in the nose and taper areas.

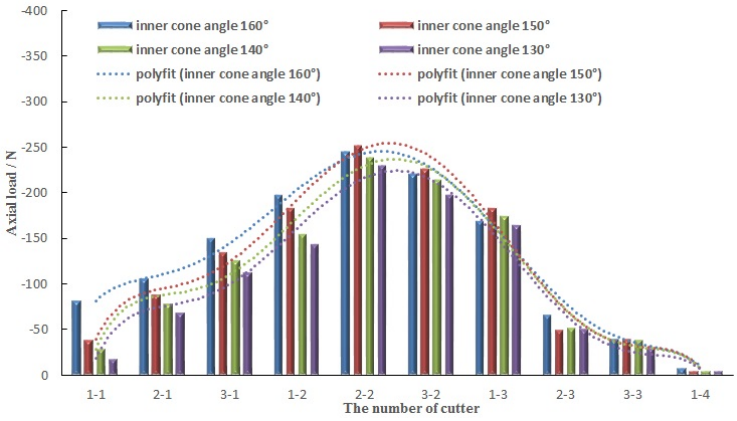

Figure 8 Histogram of the axial load on the cutters with different inner cone angles.

Figure 9 is a histogram of the radial load on the cutters along the radial direction of the bit at different inner cone angles. From Figure 9 it can be seen that cutters 1-3 and 3-3 bore maximal radial load in the shoulder area. With the decrease of the inner cone angle, the radial load on cutters 1-1, 2-1, 3-1 and 1-2 decreased gradually in the inner cone area. In all programs, the radial load on the cutters was the same in the nose and taper areas.

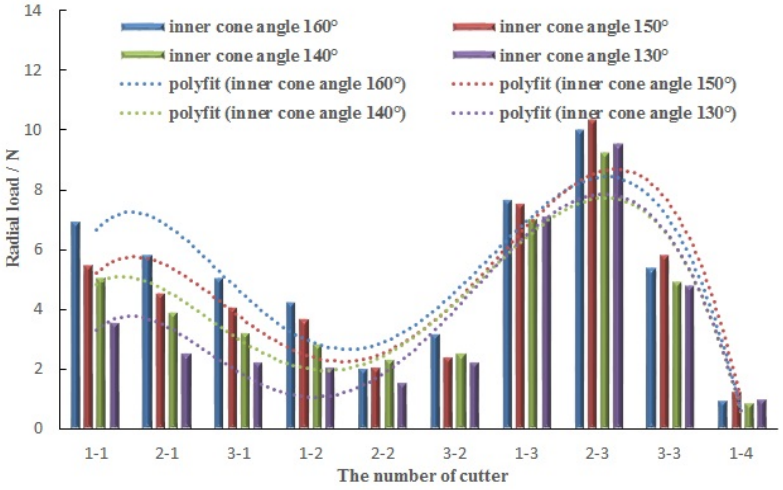

Figure 9 Histogram of the radial load on the cutters at different inner cone angles.

From the analysis above, the influence of the inner cone angle on the cutter load was mainly focused in the inner cone area. The load on the cutters in the inner cone area decreased gradually with the decrease of the inner cone angle.

3.2.2 Influence of Outer Arc Radius on Cutter Load

Leaving the inner cone angle of 130° unchanged, the outer arc radius was taken as 25 mm, 20 mm, 18 mm and 15 mm respectively. Figure 10 shows a histogram of the axial load on the cutters along the radial direction of the bit for different outer arc radii.

From Figure 10 it can be seen that, cutters 2-2 and 3-2 bore maximal axial load in the nose and taper areas. With the decrease of the outer arc radius, the axial load on cutters 1-2, 2-2, 3-2 and 1-3 decreased gradually in the nose and taper areas. In all programs, the axial load on the cutters was the same in the inner cone and shoulder areas.

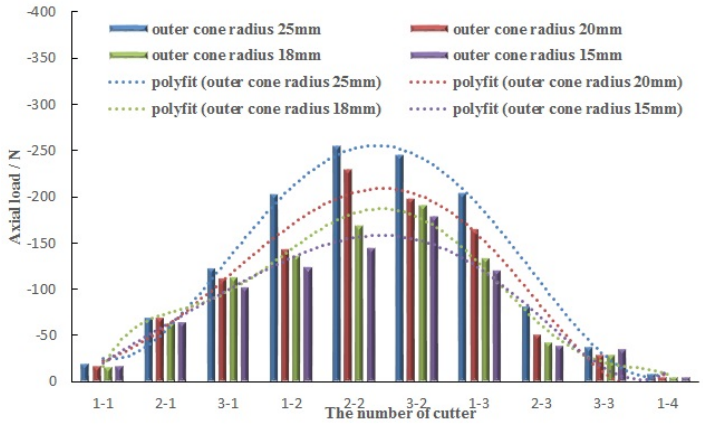

Figure 10 Histogram of axial load on the cutters for different outer arc radii.

Figure 11 shows a histogram of the radial load on the cutters along the radial direction of the bit for different outer arc radii. From Figure 11 it can be seen that cutters 1-3, 2-3 and 3-3 bore maximal radial load in the shoulder area. With the decrease of the outer arc radius, the radial load on cutters 2-2, 3-2, 1-3 and 2-3 decreased gradually in the nose and taper areas. In all programs, the radial load on the cutters was the same in the inner cone area.

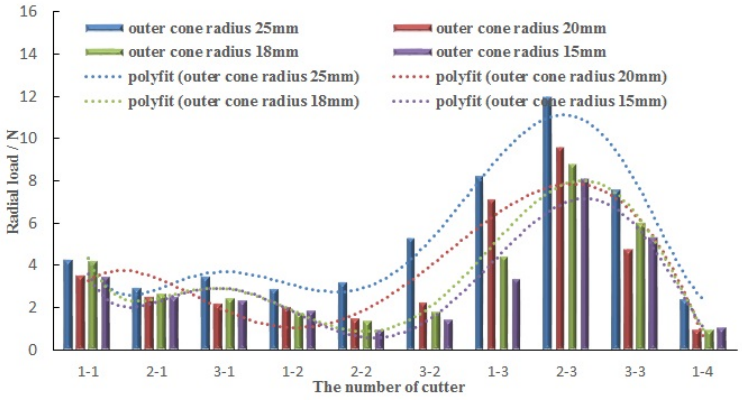

Figure 11 Histogram of the radial load on the cutters for different outer arc radii.

From the above analysis, the influence of the outer arc radius on the cutter load was mainly focused in the nose and taper areas. With the decrease of the outer arc radius, the load on the cutters decreased gradually in the nose and taper areas.

3.2.3 Optimal Design of the Crown Shape

The axial load on the cutters in the nose and taper areas was larger than in the case of the other cutters, while the radial load on the cutters in the inner cone and shoulder areas was larger than in the case of the other cutters. On the one hand, it is beneficial to decrease the rock-breaking load on the cutters in the inner cone area by decreasing the inner cone angle. On the other hand, it helps to decrease the rock-breaking load on the cutters in the nose and taper areas by decreasing the outer arc radius. Hence, in an optimal design of the bit crown shape, the inner cone angle and outer arc radius should be as small as possible in order to decrease the load on the cutters, and reduce the uneven load distribution degree.

However, it is important to note that the inner cone angle and outer arc radius should not be too small. Too small an inner cone angle will restrict the placement of the cutters at the center of the bit. Also, the smaller the outer arc radius, the steeper the crown shape in the nose and taper areas, so stress concentration is easily formed and hence the cutters are easily broken in these areas. On the basis of the above analysis, for an optimal design of the crown shape of the complex curve PDC bit, the inner cone angle was set to 130° and the outer arc radius was set to 18 mm.

4 Field Test

A ø94 mm complex curve PDC bit was designed and produced according to the optimization result. A field test was carried out in the Sihe Zhaozhuang coal mine field. The lithology of the stratum was mainly siltstone and fine sandstone, and the rock solid coefficient was around 8. The drill rig used was a ZDY1900S split hydraulic drill rig and the drill pipe was a ø73/63.5 mm auger stem. The cumulative used number of new designed ø94 mm complex curve PDC bits was 4. Figure 12 shows an image of the used new designed complex curved PDC bit. From the photo is can be seen that the wear of the cutters mainly occurred in the bit nose and taper areas of blades 2 and 3. The wear of the other cutters was relatively slight. Table 2 provides the specific drilling data of the tested complex curved PDC bits.

The average footage and average drilling efficiency of the four bits were 2030 m and 65 m/h. For hard rock, the average drilling efficiency was 9 m/h. For the original complex curved PDC bit used in the same field, the average footage and drilling efficiency were 1668 m and 55 m/h, and the average drilling efficiency for hard rock is 6 m/h.

Figure 12 Photo of new designed complex curved PDC bit.

Table 2 Field drilling data.

Bit	Accumulated drill hole number	Accumulated footage (m)	Average drilling efficiency (m/h)	Average drilling efficiency of hard rock (m/h)	Bit wear condition
XAL K01	61	1542	30	10	The wear height of cutters 2-2 and 3-2 was 3 mm, the other cutters' wear height was less than 1 mm
XAL K02	86	2566	30	9	The wear height of cutter 2-2 was 4 mm, the other cutters' wear height was less than 1 mm
XAL K03	66	2417	35	8	Cutter 3-2 was delaminated, the other cutters' wear height was less than 1 mm
XAL K04	39	1596	35	9	The wear height of cutter 3-2 was 3.5 mm, the other cutters' wear height was less than 1 mm

Compared with the original complex curved PDC bit, the average bit life and drilling efficiency of the new designed complex curved PDC bit was increased by 20% and 18% respectively. For hard-rock drilling, the drilling efficiency was increased by 50%. Hence, for hard-rock drilling, the new designed complex curved PDC bit can improve bit life and drilling efficiency remarkably.

5 Conclusion

To solve the problem that the wear of the complex curved PDC bit is uneven, the cutter load distribution law and the optimal design of the crown shape of the complex curved PDC bit were investigated based on the finite element method. In the simulation, a single cutter was taken as the research object. The rock was set as an elastic-plastic damage constitutive Cambridge material, while the cutter was set as a rigid material.

The simulation results showed that along the radial direction of the bit, the axial load on the cutters increased first and then decreased, while the radial load on the cutters decreased first and then increased; the influence of the inner cone angle on the cutter load was focused in the bit inner cone area, while the influence of the outer arc radius on the cutter load was focused in the bit nose and taper areas. The load on the cutters decreased gradually in the bit's inner cone area with the decrease of the inner cone angle, while the load on the cutters in the bit nose and taper areas decreased gradually with the decrease of the outer arc radius.

The field-test results showed that the new designed complex curved PDC bit had longer bit life and higher drilling efficiency; especially for hard-rock drilling the advantage is obvious.

Acknowledgements

This research was supported by the Fundamental Research Funds of National Natural Science Foundation of China (Grant Nr. 51774320) and the Fundamental Research Funds of TIANDI Science & Technology Co., LTD (grant number 2018-TD-QN053). The author gratefully acknowledges the financial support of both organizations.

References

[1] Xiaoliang, G., Hongyan, C. & Peng, Z., *Research on Diamond Bits for Coal Mine Drilling in Hard Formations*, Equipment for Geotechnical Engineering, **15**(3), pp. 15-18, 2014.

[2] Xianzhen, Z., Chuanliu, W. & Gang, L., *Research and Application of Curved Structure Drill in Qinglong Coal Mine*, Diamond & Abrasive Engineering, **35**(4), pp. 66-69, 2015.

[3] Rongjun, S., Shuancheng, G., Pei, J. & Ke G., *Optimal Design of New Arc Angle PDC Drill Bit for Coal Mining Based on Finite Element Method*, Journal of Jilin University (Engineering and Technology Edition), **47**(6), pp. 1991-1998, 2017.

[4] Alpak, F.O., Berg, S. & Zacharoudiou, I., *Prediction of Fluid Topology and Relative Permeability in Imbibition in Sandstone Rock by Direct Numerical Simulation*, Advances in Water Resources, **122**, pp. 49-59, 2018.

[5] Chunliang, Z., Yingxin, Y., Min, L. & Lian C., *Research on Rock-Breaking Mechanism of Cross-Cutting PDC Bit*, Journal of Petroleum Science and Engineering, **161**, pp. 657-666, 2018.

[6] Singarimbun A., Gaffar E.Z. & Tofani, P., *Modeling of Reservoir Structure by Using Magnetotelluric Method in the Area of Mt. Argopuro, East Java, Indonesia*, Journal of Engineering & Technological Sciences, **49**(6), pp.833, 2017.

[7] Jayasinghe, L.B., Zhou, H.Y. & Goh, A.T.C., Zhao Z.Y. & Gui Y.L., *Pile Response Subjected to Rock Blasting Induced Ground Vibration Near Soil-Rock Interface*. Computer and Geotechnics, **82**, pp. 1-15, 2017.

[8] Feng, Y., Arlanoglu, C., Podnos, E., Becker E. & Gray K.E., *Finite-Element Studies of Hoop-Stress Enhancement for Wellbore Strengthening*, SPE Drilling & Completion, **30**(1), pp. 38-51, 2015.

[9] Reyes Martinez, I., Fontoura, S., Inoue, N., Carraoatoso, C., Lourengo, A. & Curry, D., *Simulation of Single Cutter Experiments in Evaporites Through Finite Element Method*, SPE/IADC Drilling Conference, Society of Petroleum Engineers, 2013.

[10] Jaime, M.C., Gamwo, I.K., Lyons, D.K. & Lin, J.S., *Finite Element Modeling of Rock Cutting*, 44th US Rock Mechanics Symposium and 5th US-Canada Rock Mechanics Symposium, American Rock Mechanics Association, Salt Lake City, UT, 2010.

[11] Zhou, Y., Jaime, M.C., Gamwo, I.K., Zhang, W. & Lin, J.S., *Modeling Groove Cutting in Rocks Using Finite Elements*, 45th US Rock Mechanics/Geomechanics Symposium, American Rock Mechanics Association, 2011.

[12] Pryhorovska, T.O., Chaplinskiy, S.S. & Kudriavtsev, I.O., *Finite Element Modelling of Rock Mass Cutting by Cutters for PDC Drill Bits*, Petroleum Exploration and Development, **42**(6), pp. 888-892, 2015.

[13] Hongxiang, J., Zenghui, L. & Kuidong, G., *Numerical Simulation on Rock Fragmentation by Discontinuous Water-Jet Using Coupled SPH/FEA Method*. Powder Technology, **312**, pp. 248-259, 2017.

[14] Ducobu, F., Rivière-Lorphèvre, E. & Filippi, E., *Finite Element Modelling of 3D Orthogonal Cutting Experimental Tests with The Coupled Eulerian-Lagrangian (CEL) Formulation*, Finite Elements in Analysis and Design, **134**, pp. 27-40, 2017.

[15] Linwei, D., Mingyi, Z., Yunyun, X., Mengmeng L., Jianxing X. & Lanxia C., *Study on the Parameters of Soil Models Yield Criterion in ABAQUS Software*, Journal of Qingdao Technological University, **34**(1), pp. 48-50, 2013.